

# Nitroxide-Mediated Polymerization of Styrene Initiated from the Surface of Silica Nanoparticles. In Situ Generation and Grafting of Alkoxyamine Initiators

C. Bartholome,<sup>†,‡</sup> E. Beyou,<sup>‡</sup> E. Bourgeat-Lami,<sup>\*,†</sup> P. Chaumont,<sup>‡</sup> F. Lefebvre,<sup>§</sup> and N. Zydziewicz<sup>‡</sup>

Laboratoire de Chimie et Procédés de Polymérisation, UMR 140 CNRS, CPE, Bât. 308F, BP2077, Laboratoire des Matériaux Polymères et des Biomatériaux, UMR 5627 CNRS, UCBL, Bât. ISTIL, and Laboratoire de Chimie Organométallique des Surfaces, CPE, Bât. 308F, BP2077, 43 Bd. Du 11 Nov. 1918, 69616 Villeurbanne Cedex, France

Received July 22, 2004; Revised Manuscript Received November 27, 2004

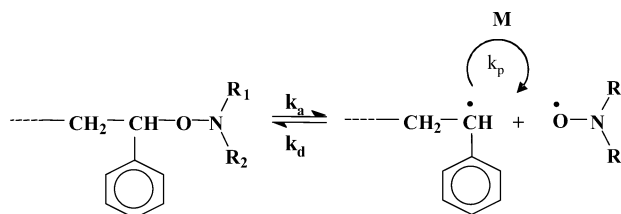
**ABSTRACT:** Polystyrene (PS)-grafted silica nanoparticles were prepared by nitroxide-mediated polymerization of styrene using *N-tert-butyl-N*-[1-diethylphosphono(2,2-dimethylpropyl)] nitroxide (DEPN) as mediator. Two routes were investigated to graft the alkoxyamine initiator onto silica. In the first route, (acryloxypropyl)trimethoxysilane (APTMS) was covalently attached to silica and the alkoxyamine was formed in situ by spin trapping the acryloxy radicals produced by reaction of azobisisobutyronitrile (AIBN) with the grafted APTMS molecules using DEPN as radical trap. In the second route, the surface alkoxyamine initiator was produced in a one-step process by reacting *simultaneously* DEPN, AIBN, and APTMS in the presence of silica. Next, polystyrene chains with controlled molecular weights and narrow polydispersities were grown from the alkoxyamine-functionalized nanoparticle surface. The amount of polystyrene grafted to the surface was determined by thermogravimetric analysis, and was found to increase with increasing grafting density of the alkoxyamine initiator. The resulting PS-grafted silica particles exhibited better colloidal stability and enhanced dispersability in toluene, a good solvent for polystyrene.

## Introduction

Tailoring the surface properties of mineral substrates is important in situations where interfaces play a dominant role, such as colloidal stabilization and nanocomposite materials preparation.<sup>1</sup> Therefore, the development of grafting strategies is of great current interest. Grafting can be accomplished in a number of ways, including by growth of polymer chains “from” a solid surface using immobilized initiators<sup>2–4</sup> (“grafting-from” technique), or by covalent attachment of preformed polymers to reactive sites on an inorganic surface (“grafting-to” technique).<sup>5</sup> In parallel, the growing demand for well-defined functionalized materials has led to the development of robust methodologies to precisely control the physical structure of the grafted polymer layer. Among the different methods (e.g., anionic,<sup>6</sup> cationic,<sup>7</sup> and anionic-coordinated<sup>8</sup> ring-opening polymerizations), controlled free radical polymerization (CRP) has attracted considerable attention due to its simplicity and versatility compared to ionic processes.<sup>9</sup> CRP is usually divided into three categories: atom-transfer radical polymerization (ATRP), reversible radical addition–fragmentation chain transfer (RAFT), and nitroxide-mediated polymerization (NMP). All three techniques permit the polymer molecular weight, the polydispersity, and the polymer architecture to be accurately controlled, and have recently been used to build up highly dense polymer brushes from planar substrates<sup>10</sup> or nanoparticles.<sup>11–13</sup>

We describe in this work the controlled growth of polystyrene (PS) chains from silica nanoparticles using

the “grafting-from” approach combined with the NMP technique. The key reaction of NMP is an activation/deactivation process involving a reversible combination of propagating radicals with nitroxide free radicals as schematically represented below:



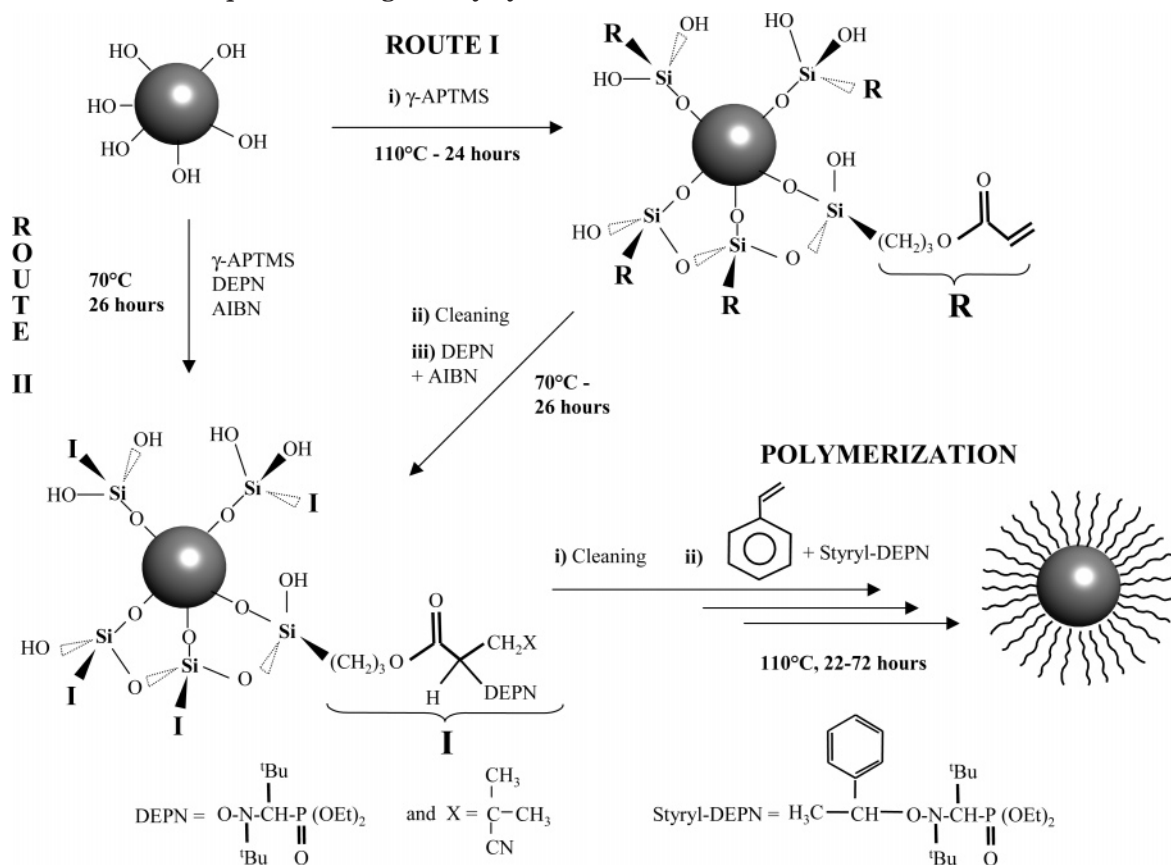
Although a library of nitroxide and nitroxide-based alkoxyamine compounds have been recently reported in the literature for the living free radical polymerization of a variety of monomers,<sup>14–16</sup> grafting of inorganic surfaces by NMP requires the development of adequate surface-active initiators and has been much less explored.<sup>17–20</sup> Reactive unimolecular alkoxyamine initiators carrying trichlorosilyl<sup>17,18</sup> or triethoxysilyl<sup>19</sup> end groups have been synthesized, and successfully employed in the growth reaction of polymer chains with controlled molecular weights and well-defined architectures from silica surfaces.<sup>17–19</sup> One of the prime advantages of these unimolecular systems is the possibility to accurately control the structure and concentration of the initiating species. However, a major drawback is the multistep synthesis of the functional alkoxyamine.<sup>20</sup> Thus, Parvole<sup>21</sup> and Kasseh<sup>22</sup> reported a bimolecular system based on the strategy of R  he<sup>2–4</sup> in which the NMP process is initiated from an azo or a peroxide initiator attached to fumed silica. While successful, this approach still involves a two-step synthesis of the

\* To whom correspondence should be addressed.

<sup>†</sup> Laboratoire de Chimie et Proc  d  s de Polym  risation, CPE.

<sup>‡</sup> Laboratoire des Mat  riaux Polym  res et des Biom  t  riaux, UCBL.

<sup>  </sup> Laboratoire de Chimie Organom  tallique des Surfaces, CPE.

**Scheme 1. Reaction Scheme for Covalent Bonding of the DEPN-Based Alkoxyamine Initiator onto Silica and Subsequent Grafting of Polystyrene from the Functionalized Silica Surface**

functional azoic or peroxidic initiator. Therefore, the need for a versatile and easy “one-step” grafting procedure has motivated us to find an alternative method to chemically attach the alkoxyamine initiator onto the mineral surface. Our strategy relies on the use of a silane coupling agent bearing a terminal double bond: (acryloxypropyl)trimethoxysilane (APTMS). The reaction of azobisisobutyronitrile (AIBN) with the double bond of the APTMS molecule creates radical intermediates that are trapped in situ by *N*-*tert*-butyl-*N*-[1-diethylphosphono(2,2-dimethylpropyl)] nitroxide (DEPN), leading to a surface alkoxyamine. Although (acryloxypropyl)- and (methacryloxypropyl)trialkoxysilanes have already been reported to be suitable coupling agents for the elaboration of polymer/silica nanocomposite colloids through dispersion and emulsion polymerizations,<sup>23,24</sup> to the best of our knowledge, there is no precedent in the literature on the utilization of such monomeric silanes for the synthesis of surface alkoxyamine initiators. Among the different polymerizable silanes commercially available, APTMS combines two advantages. First, it contains a cleavable ester group that will enable us to quantitatively separate the grafted polymer chains from the surface and experimentally determine their molecular weights, and second, we can expect efficient trapping of the intermediate acryloxy radicals by DEPN without the occurrence of undesirable side reactions.

To produce nanoparticles with a high density of grafts, we first optimized the conditions for grafting the alkoxyamine initiator on the silica surface. The NMP of styrene from the grafted alkoxyamine was then examined in depth, and a correlation was established between the polymer grafting density and the initial

concentration of the alkoxyamine initiator. Finally, DLS measurements and TEM analysis were performed on the PS-grafted silica suspensions to examine the influence of the extent of grafting on the properties of the composite particles.

## Experimental Section

**Materials.** Fumed silica (Aerosil A200V, Degussa) with an average diameter of 13 nm and a specific surface area of 228 m<sup>2</sup>/g was dried for 4 h at 150 °C under a vacuum before use. Styrene (99%, Aldrich) and toluene (99.3%, Aldrich) were vacuum distilled on molecular sieves before use. AIBN (98%, Acros Organics) was recrystallized from methanol. APTMS (95%, Gelest) was used as supplied. DEPN (88%) was kindly supplied by Atofina, and used as received. The free initiator, a DEPN-based alkoxyamine (styryl-DEPN, Scheme 1), was prepared using a procedure described in the literature.<sup>25</sup>

**Initiator Attachment on the Silica Surface (Scheme 1). Route I.** In a typical run, 1.28 g of APTMS (5.5 mmol or 12  $\mu\text{mol}/\text{m}^2$ ) was added to a suspension of silica (1.9 g) in toluene (48 g) and stirred for 30 min at room temperature. The mixture was heated to 110 °C for 24 h. The free nongrafted APTMS was discarded by successive centrifugation/redispersion cycles, and the recovered grafted silica powder was dried in a vacuum oven at 50 °C before analysis. The alkoxyamine was formed in situ by introducing 0.28 g of AIBN (1.7 mmol) and 1.16 g of DEPN (3.95 mmol) into 93 g of toluene containing 1.9 g of the APTMS-grafted silica. The suspension was degassed by four freeze–pump–thaw cycles, and the mixture was heated to 70 °C for 26 h to yield the surface alkoxyamine.

**Route II.** In a second route, the surface-tethered alkoxyamine initiator was produced in one step by adding *simultaneously* APTMS (1.28 g, 5.47 mmol), AIBN (0.43 g, 2.62 mmol), and DEPN (1.74 g, 5.9 mmol) into a suspension of raw silica (1.9 g) in toluene (93 g). The grafting was performed at 70 °C for 26 h as above. The resulting alkoxyamine-grafted silica was

extensively washed by a series of centrifugations/redispersions in toluene, dried under vacuum at 50 °C, and characterized by solid-state nuclear magnetic resonance (NMR) and Fourier transform infrared (FTIR) spectroscopies. The alkoxyamine grafting density was determined by TGA and phosphorus elemental analysis.

**Stable Free Radical Polymerization of Styrene from the Functionalized Silica Surface.** In a typical run, 0.3 g of the alkoxyamine-functionalized silica (amount of surface alkoxyamine 0.05 mmol), toluene (14.70 g, 0.16 mol), styrene (15.50 g, 0.15 mol), and the required amount of the “free” alkoxyamine initiator (0.05 g, 0.14 mmol), corresponding to a constant styrene-to-initiator molar ratio of around 800, were introduced in a predried Schlenk flask under an argon atmosphere. After being stirred for a few minutes, the suspension was degassed by four freeze–pump–thaw cycles, and the polymerization mixture was heated to 110 °C for 54 h. The conversion (53%) was determined gravimetrically. The PS-grafted silica particles (1.2 g) were characterized by transmission electron microscopy (TEM) and dynamic light scattering (DLS).

**Recovery of the Free and Grafted Polymer Chains.** The free polymer, formed in solution, was isolated from the grafted silica particles by exhaustive cleaning by a series of centrifugation/redispersion cycles in toluene. In a typical example, 30 mL of the silica suspension was centrifuged at 18000 rpm (Beckman Avanti 30) for 20 min. After each cycle, the solvent was discarded and replaced by an equivalent volume of fresh toluene. The polymer content of the supernatant cleaning solutions (determined gravimetrically) decreased from 38 to 0 wt % after six cycles, indicating complete removal of the physisorbed polymer chains from the surface. Then, the free polymer (7.4 g) obtained after precipitation of the supernatant in MeOH and the recovered PS-grafted silica powder (1.2 g) were collected separately and dried at 50 °C for 4 h and at 60 °C overnight, respectively, prior to characterization. TGA was used to assess the amount of grafted polymer onto silica. Degrafting of the polystyrene chains from the silica surface was performed as reported previously.<sup>16</sup> Namely, 150 mg of the polymer-modified silica gel was suspended in 30 mL of toluene. Then, 3 mL of MeOH and 15 mg (0.08 mmol) of *p*-toluenesulfonic acid monohydrate were added to the grafted silica suspension, and the mixture was heated to reflux overnight. The polystyrene chains, cleaved from the surface, were finally isolated as described above for nonbonded polymer. Molecular weights of free and grafted polymers were determined by size exclusion chromatography (SEC).

**Characterization.** <sup>29</sup>Si and <sup>13</sup>C solid-state NMR were performed on a Bruker DSX-300 spectrometer operating at 59.63 and 75.47 MHz, respectively, by use of cross-polarization from a proton. The contact time was 5 ms, the recycle delay 1 s, and the spinning rate 10 kHz. The <sup>29</sup>Si MAS NMR spectra were referenced to tetramethylsilane. SEC analysis was performed at 45 °C using a 410 Waters differential refractometer, a 996 Waters photodiode array detector, a 717 Waters autosampler, a 515 Waters HPLC pump, a set of two Waters microstyragel columns (HR1 and HR4, weight range 5000–600000), and THF as eluent (1 mL/min). Polymer molecular weights were derived from a calibration curve based on polystyrene standards.

Infrared spectra were recorded using a Nicolet FTIR 460 spectrometer on powder-pressed KBr pellets. The hydroxyl region was observed on samples made of self-supporting wafers of around 20 mg/cm<sup>2</sup> previously dried under vacuum at 50 °C for 4 h. TGA was carried out using a Mettler TG 50/TA 3000 thermobalance, controlled by a TC10A microprocessor. Samples were heated at 10 °C/min under a nitrogen flow (150 mL/min). The grafting density was determined using eq 1,

$$\text{grafting density } (\mu\text{mol}/\text{m}^2) = \frac{\left( \frac{W_{60-730}}{100 - W_{60-730}} \right) \times 100 - W_{\text{silica}}}{MS_{\text{spec}} \times 100} \times 10^6 \quad (1)$$

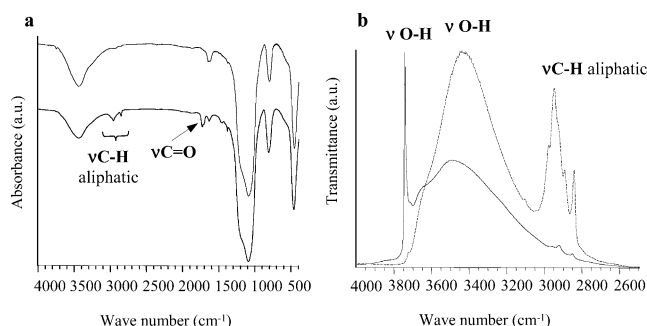


**Figure 1.** (a) FTIR spectra of the Aerosil A200V silica particles before (top) and after (bottom) APTMS grafting, and (b) enlargement of the FTIR spectra of the hydroxyl region of the A200V silica before grafting (full line) and after grafting (dotted line). APTMS grafting density 2.1  $\mu\text{mol}/\text{m}^2$ .

where  $W_{60-730}$  is the weight loss from 60 to 730 °C corresponding to the decomposition of the silane, the alkoxyamine, or the polystyrene,  $M$  (g/mol) is the molar mass of the degradable part of the grafted molecule, and  $S_{\text{spec}}$  (m<sup>2</sup>/g) and  $W_{\text{silica}}$  are, respectively, the specific surface area and the weight loss of silica determined before grafting.

The grafting yield, which corresponds to the fraction of APTMS effectively attached to the silica surface, was determined using the following formula:

$$\text{APTMS grafting yield (\%)} = \frac{\text{grafting density} \times 100}{[\text{APTMS}]} \quad (2)$$

where [APTMS] ( $\mu\text{mol}/\text{m}^2$ ) designates the initial concentration of the silane molecule.

As an alternative to TGA, the alkoxyamine grafting density was also determined by elemental analysis from the phosphorus content ( $P$ , wt %) using eq 3, where  $M$  designates the molar mass of the grafted alkoxyamine molecule ( $M = 552$  g/mol) and  $S_{\text{spec}}$  (m<sup>2</sup>/g) has the same meaning as previously.

$$\text{alkoxyamine grafting density } (\mu\text{mol}/\text{m}^2) = \frac{10^6 P}{[(3100 - P(M - 1))S_{\text{spec}}]} \quad (3)$$

In a typical analysis, the silica powder was mineralized by dissolution in a mixture of strong acids and the phosphorus content was titrated by inductively coupled plasma atomic emission spectroscopy (ICP AES). TEM analysis was performed on a Philips CM10 electron microscope operating at 80 kV. In a typical experiment, one drop of the colloidal dispersion was put on a carbon film supported by a copper grid and allowed to air-dry before observation. Particle size was determined by DLS at 670 nm using a Malvern autosizer Lo-c apparatus with a detection angle of 90°. The measurements were carried out at 23 °C on highly diluted samples to rule out interaction and multiple scattering effects. The intensity average diameter was computed from the intensity autocorrelation data using the cumulant analysis method.<sup>26</sup>

## Results and Discussion

**APTMS Grafting onto Aerosil.** Preliminary experiments performed on APTMS alone enabled us to determine the optimal conditions for grafting of the silane molecule. The grafting was qualitatively evidenced by FTIR and solid-state NMR spectroscopies, which attested for covalent attachment of the silane units on the surface. The FTIR spectra of Aerosil and APTMS-decorated silica are reported in Figure 1a. Characteristic vibrations of the carbonyl ( $\nu_{\text{C=O}}$  1750 cm<sup>-1</sup>) and the aliphatic ( $\nu_{\text{CH}}$  2800–3000 cm<sup>-1</sup> and  $\delta_{\text{CH}}$  1350 cm<sup>-1</sup>) groups of the APTMS molecule appear after grafting. The FTIR spectrum of the hydroxyl region of silica (Figure 1b) exhibits a strong OH stretching vibration



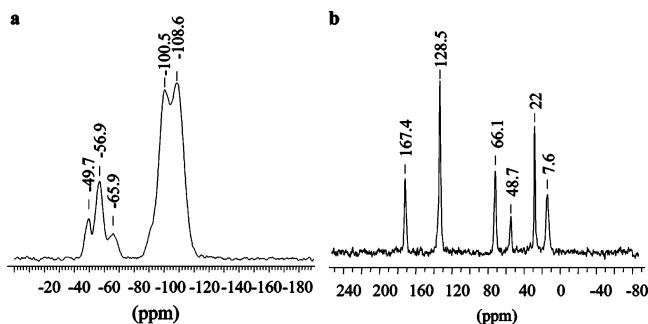


**Figure 2.** (a)  $^{29}\text{Si}$  and (b)  $^{13}\text{C}$  CP-MAS solid-state NMR spectra of the APTMS-functionalized silica particles. APTMS grafting density  $2.1 \mu\text{mol}/\text{m}^2$ .

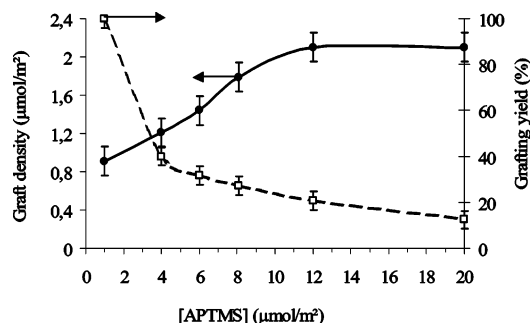


**Figure 3.** APTMS grafting density and grafting yield as a function of the APTMS concentration. Silica concentration 3.8 wt % in toluene. Temperature  $110^\circ\text{C}$ . Reaction time 24 h.

band in the range  $3600\text{--}3100 \text{ cm}^{-1}$  due to physisorbed water and hydrogen-bonded silanol groups, and a sharp peak at  $3740 \text{ cm}^{-1}$  corresponding to terminal nonreacted silanols. The latter peak disappeared after grafting, while new bands corresponding to aliphatic carbons appeared in the  $3000\text{--}2800 \text{ cm}^{-1}$  region consistent with grafting.<sup>27</sup>

The  $^{29}\text{Si}$  CP-MAS spectrum (Figure 2a) shows two sets of resonances in the ranges  $-90$  to  $-110$  and  $-50$  to  $-70$  ppm. The first group is characteristic of silica and corresponds to  $\text{Q}^4$  [ $\text{Si}(\text{OSi})_4$ ,  $-108$  ppm] and  $\text{Q}^3$  [ $\text{Si}(\text{OSi})_3\text{OH}$ ,  $-100$  ppm] species. The second group is not observed for raw silica, and clearly attests that a grafting reaction occurred between APTMS and Aerosil. The three peaks at  $-49$ ,  $-57$ , and  $-66$  ppm are characteristic of  $\text{T}^{3-n}$  species [ $\text{Si}(\text{OSi})_{3-n}(\text{OH})_n\text{R}$ ] ( $n = 0\text{--}2$ , respectively), where R designates the organic part of the silane compound, and show that various species had formed on silica. The  $^{13}\text{C}$  NMR spectrum of Figure 2b indicates the presence of remaining methoxy groups (peak at  $48.7$  ppm) while the other peaks are in agreement with the structure of grafted APTMS.

Figure 3 shows the evolution of the grafting density and of the grafting yield (determined by TGA) as a function of the silane concentration. The grafting density increases with increasing silane content and reaches a plateau at high concentrations while, concurrently, the grafting yield decreases. In agreement with the literature data,<sup>28</sup> a maximum grafting density of  $2.1 \mu\text{mol}/\text{m}^2$ , corresponding to a monolayer coverage, was achieved for a silane content of  $12 \mu\text{mol}/\text{m}^2$ .

**Coupling Reaction of DEPN and AIBN with Grafted APTMS (Route I).** The reaction of DEPN and AIBN with the grafted APTMS molecules is expected to give a large number of products,<sup>15</sup> among which the surface alkoxyamine can be readily isolated by sedi-

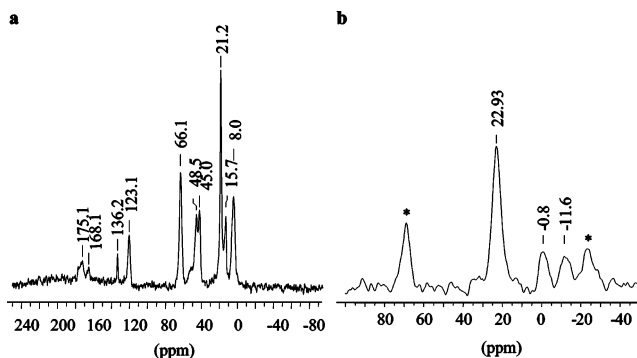


**Figure 4.** (a)  $^{13}\text{C}$  and (b)  $^{31}\text{P}$  CP-MAS solid-state NMR spectra of the alkoxyamine-functionalized silica particles (route I). Asterisks indicate rotational bands. Alkoxyamine grafting density  $0.5 \mu\text{mol}/\text{m}^2$ .

mentation of silica and cleaning of the surface.  $^{31}\text{P}$  and  $^{13}\text{C}$  NMR spectroscopies both indicated successful formation of the alkoxyamine initiator. The  $^{13}\text{C}$  NMR spectrum of Figure 4a exhibits all the characteristic signals of the alkoxyamine compound. The chemical shift at  $66$  ppm can be assigned to the methylene carbon of the ethoxy groups of the DEPN moiety and to the ethylene carbon of the propoxy group of APTMS, while the peak at  $136$  ppm corresponds to the carbon of the nitrile group of AIBN. The signals at  $48$ ,  $45$ ,  $21$ ,  $16$ , and  $7$  ppm are attributed to aliphatic carbons. In addition, the spectrum indicates two chemical shifts for the carbonyl group at  $175$  and  $168$  ppm. The former corresponds to grafted APTMS, while the latter may be due to nonreacted APTMS molecules. As a matter of fact, residual ethylenic carbons can be identified at  $123$  ppm, giving a clear confirmation of the presence of nonreacted double bonds.

The  $^{31}\text{P}$  solid-state NMR spectrum of Figure 4b shows three peaks at  $23$ ,  $-1$ , and  $-12$  ppm. The peak at  $23$  ppm corresponds to more than  $80\%$  of the total intensity. It can be attributed to the phosphoric atom of the DEPN moiety ( $\delta = 23\text{--}24$  ppm in solution),<sup>29</sup> and indicates that the reaction occurred mainly as expected. The two peaks at  $-1$  and  $-12$  ppm may correspond to byproducts of commercial DEPN, whose purity is only  $88\%$ , while the last two signals can be attributed to rotational bands of the peak at  $23$  ppm.

To gain insight into the grafting process and accurately determine the grafting density of the initiator units on the surface, we performed a quantitative analysis by TGA. The density of the initiator units, determined by this method, was around  $0.5 \mu\text{mol}/\text{m}^2$ . This value is lower than the value reported in our previous work on the grafting of a triethoxysilyl-terminated alkoxyamine, for which we determined an optimum grafting density of around  $0.9 \mu\text{mol}/\text{m}^2$ .<sup>19</sup> However, we can reasonably assume that, in the present work, addition of the AIBN radicals to the double bond of the grafted APTMS molecule competes with trapping of these radicals by DEPN, which can affect the grafting efficiency. In addition, as shown by  $^{13}\text{C}$  NMR analysis, only part of the APTMS molecules were involved in the coupling reaction. Indeed, previously attached alkoxyamine initiators may prevent further access of the bulky DEPN nitroxide radicals to neighboring APTMS molecules, a scenario which may also account for the observed low grafting density. Next, polymer chains were grown from the silica surface under conditions similar to those reported previously (i.e., using a 50/50

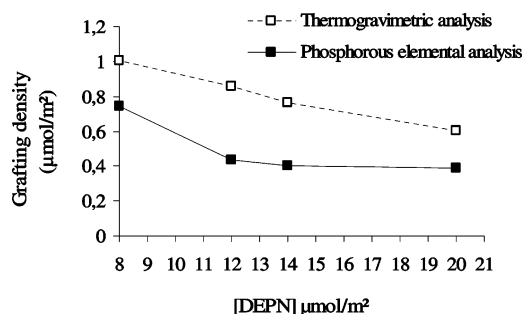


**Figure 5.** Alkoxyamine grafting densities as a function of DEP.N concentration (route II). Silica concentration 2 wt % in toluene. (Acryloxypropyl)trimethoxysilane concentration 12  $\mu\text{mol}/\text{m}^2$ . Azobisisobutyronitrile concentration 6  $\mu\text{mol}/\text{m}^2$ . Temperature 70 °C. Reaction time 26 h.

v/v mixture of styrene and silica suspension together with a known amount of free alkoxyamine initiator corresponding to a styrene to initiator molar ratio of 800). As a direct consequence of the low amount of initiating species attached to silica, the TGA results indicated a very low concentration of grafted polymer chains (typically around 0.08  $\mu\text{mol}/\text{m}^2$ ), which corresponds to less than 20% initiation efficiency. Although it is known from previous studies that not all of the initiator sites grafted to the surface participate in the growth reaction, the above value corresponds to a low efficiency compared to the literature data (typical efficiencies are in the range 30–50 mol %).<sup>12,19,22</sup> Several hypotheses have been formulated to account for the loss of initiating groups during controlled radical polymerizations from inorganic surfaces, but one of the most probable issues involves a termination reaction between a growing polymer chain and a surface-bound polymer. It is clear that such a termination mode will be promoted under conditions which favor the access of the propagating radicals to the surface, and in particular for a low initial amount of grafted polymer chains.

**In Situ Synthesis of the Surface Alkoxyamine Initiator (Route II).** To overcome the aforementioned difficulties and reach higher polymer grafting densities, we decided to generate and graft *simultaneously* the functional alkoxyamine onto silica in a one-step process by mixing together AIBN, APTMS, and DEP.N (Scheme 1). We maintained the APTMS concentration at the same level as previously (12  $\mu\text{mol}/\text{m}^2$ ) since these conditions proved to give the best grafting efficiency. The amount of AIBN was chosen to provide an equivalent molar concentration of free radicals (2AIBN/APTMS = 1) while we varied the DEP.N concentration. The coupling and simultaneous grafting reactions were conducted at 70 °C.

From a qualitative point of view, <sup>31</sup>P together with <sup>29</sup>Si and <sup>13</sup>C solid-state NMR analysis gave confirmation of grafting of the alkoxyamine initiator. The spectra were similar to those reported previously (Supporting Information). But significantly different quantitative results were obtained between the two routes: the grafting density, determined by TGA, increased from 0.5  $\mu\text{mol}/\text{m}^2$  for route I to 0.86  $\mu\text{mol}/\text{m}^2$  for route II, in the presence of the same amount of DEP.N (corresponding to 12  $\mu\text{mol}/\text{m}^2$ ). To determine the optimal alkoxyamine grafting conditions, it was next decided to vary the DEP.N loading while keeping all other parameters constant. Figure 5 shows the evolution of the alkoxyamine grafting density as a function of the DEP.N concentration (expressed in  $\mu\text{mol}/\text{m}^2$ ). The grafting

density decreases as the DEP.N concentration increases. This is presumably due to the fact that, in the presence of an excess of DEP.N, the reaction that preferentially takes place is the coupling between the radicals formed upon thermal decomposition of AIBN and the DEP.N counter-radicals. This results in a decrease of the probability of radical addition to the double bonds of the APTMS molecule, and contributes therefore to a lowering of the amount of grafted alkoxyamine.<sup>30</sup> In contrast, the grafting density increases with decreasing amount of DEP.N and reaches an upper value of around 1  $\mu\text{mol}/\text{m}^2$  for a DEP.N content of 8  $\mu\text{mol}/\text{m}^2$ , which is of the same order of magnitude as the grafting density reported in our previous work.<sup>19</sup> The fact that we reached a grafting density similar to the one achieved during the grafting of a preformed alkoxyamine, but larger than the one measured in route I, suggests that the alkoxyamine compound is formed preferentially, and subsequently grafted to the silica surface. However, we cannot completely exclude the possibility of grafting of APTMS molecules before they can undergo radical addition and coupling, an issue which would lead to overestimated values of the alkoxyamine grafting density since the silica surface would contain not only the targeted alkoxyamine compound but also residual APTMS molecules. The presence of nonreacted silane units on the surface is qualitatively evidenced by <sup>13</sup>C solid-state NMR analysis which indicates the presence of residual ethylenic carbons after grafting. All of the APTMS molecules were not converted into alkoxyamine initiators presumably for two reasons. First, as mentioned earlier for route I, previously grafted alkoxyamines may prevent access of the radicals to the surface and, second, termination reactions may occur in solution, leading to a decrease of the overall concentration of AIBN radicals, which will no longer be available for addition to the APTMS double bonds. If the above hypothesis is correct, however, eq 1, which is based on the assumption that the alkoxyamine initiator is the only product of the grafting reaction, should no longer be valid. Therefore, owing to the uncertainty in an accurate determination of the alkoxyamine grafting density by TGA, we decided to determine the actual concentration of grafted alkoxyamine by measuring directly the phosphorus content on the silica surface using eq 3. The results are plotted in Figure 5. As predicted, the grafting density determined by elemental analysis is systematically lower than the one estimated from TGA. This result definitely proves that the alkoxyamine initiator corresponds to only a fraction of the total amount of grafted molecules, the remaining part being presumably nonreacted APTMS. In addition, it is worthwhile to notice that the two curves exhibit the same trends (i.e., a decrease of the alkoxyamine grafting density with increasing DEP.N concentration), which confirms that the formation of the alkoxyamine initiator is promoted for low DEP.N concentrations.

In summary, phosphorus elemental analysis enabled us to determine with accuracy the amount of grafted alkoxyamine on the surface. A maximum grafting density of 0.75  $\mu\text{mol}/\text{m}^2$  was obtained for the lowest DEP.N concentration, which is slightly lower than the value reported in our previous work presumably because of competitive reactions (between APTMS grafting and alkoxyamine formation) occurring during this unconventional coupling and simultaneous grafting process.

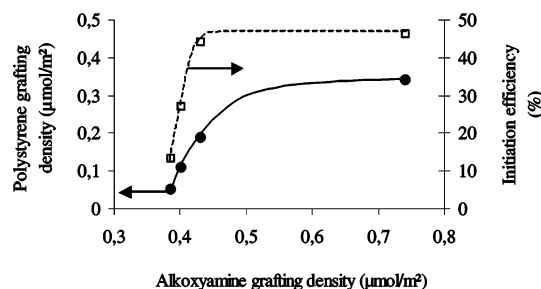
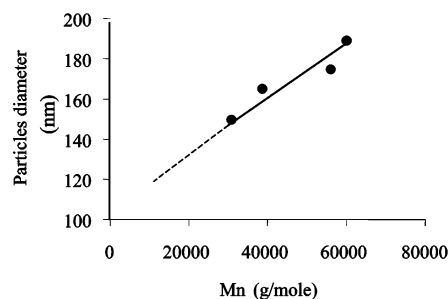
**Table 1.** Size Exclusion Chromatography Analysis of the Grafted and Free Polystyrene Chains and Grafting Densities and Particle Sizes of Polystyrene-Grafted Silica Particles for a Series of Graft-From Polymerization Reactions Performed Using Route I

run	styrene/ initiator <sup>a</sup>	time (h)	conversion (%)	$M_{n,th}^b$ (g/mol)	free polymer in solution		surface-grafted polymer		weight loss <sup>c</sup> (%)	grafting density <sup>d</sup>	particle size <sup>e</sup> (nm)
					$M_n$ (g/mol)	$M_w/M_n$	$M_n$ (g/mol)	$M_w/M_n$			
1	801	22	33	27490	30700	1.22	30900	1.22	71.3	0.33	150
2	789	33	44	36105	38400	1.21	38700	1.2	77.4	0.37	165
3	800	54	53	52416	55500	1.20	56000	1.21	80.7	0.32	175
4	806	72	64	53647	57900	1.20	60000	1.18	79.9	0.28	189

<sup>a</sup> Initiator = surface-grafted initiator + free initiator. The surface-grafted alkoxyamine concentration is equal to 0.17 mmol/g of silica, and that of the free initiator is close to 0.46 mmol/g. <sup>b</sup>  $M_{n,th} = ([M]_0/[I]_0)(M_w \text{ of styrene})(\text{conversion})/100$ . <sup>c</sup> Determined by thermogravimetric analysis. <sup>d</sup> In  $\mu\text{mol}/\text{m}^2$ —calculated using eq 1. <sup>e</sup> Determined by dynamic light scattering after removal of the free polymer chains.

**DEPN-Mediated Polymerization of Styrene from the Functionalized Silica Surface.** On the basis of previous works in the literature, and as mentioned earlier, the polymerization was performed in the presence of a known amount of “free” sacrificial initiator. The addition of free alkoxyamine creates an overall concentration of nitroxide in the polymerization mixture, which controls the chain growth of both the immobilized and soluble initiators, and allows one to achieve a good molecular weight control. We then compared the molecular weights and polydispersity indexes of the grafted and the free polymer chains for a series of growth experiments performed at a fixed styrene/initiator molar ratio and various reaction times. Table 1 indicates a good agreement between the two sets of data as already reported by many authors.<sup>12</sup> In addition, the experimental molecular weights agreed well with the theoretical ones as expected for a controlled polymerization. All these results indicate that steric constraints around silica particles have no influence on the livingness of the free radical process. From the weight loss and the  $M_n$  of PS, we can estimate the polymer chain density and compare it to the density of initiator groups reported above. The data in Table 1 indicate that a maximum polymer grafting density of around  $0.37 \mu\text{mol}/\text{m}^2$  was achieved under optimal conditions whatever the polymer molecular weight comprised between 30000 and 60000. This corresponds to approximately 40–45% initiation efficiency, which is in close agreement with the data reported by Böttcher<sup>12</sup> or Kasseh<sup>22</sup> on silica nanoparticles but is slightly lower than the data given by Ohno on gold colloids.<sup>13</sup> This suggests that chain termination reactions are promoted on the silica surface as already reported in the literature.<sup>12,22,31,32</sup> As suggested by Böttcher et al.,<sup>12</sup> this might be due to the close proximity of the propagating “living” radicals. But, according to Patten, this most likely can be ascribed to the termination between a free chain formed in solution and a surface-bound polymer.<sup>31</sup>

Next, we examined the influence of the initial alkoxyamine concentration on the polymer grafting density and on the initiation efficiency (Figure 6). As expected, the polymer grafting density increases with increasing density of grafted alkoxyamine initiator. But more interesting is the evolution of the initiation efficiency. The larger the initial amount of grafted alkoxyamine, the higher the fraction of initiator that effectively participates in the polymerization, or in other words the less important are termination reactions. Indeed, increasing the alkoxyamine grafting densities increases the polystyrene concentration, which in turn reduces the probability of chain termination because of the steric hindrance exerted by the grafted polymer chains on the surface: the dormant polymer prevents

**Figure 6.** Polystyrene grafting density and initiation efficiency as a function of the grafting density of the alkoxyamine initiator (route II). Styrene/initiator = 800. Initiator = surface-grafted initiator + free initiator. Temperature 110 °C. Reaction time 54 h.**Figure 7.** Hydrodynamic diameter of the polystyrene-grafted silica particles as a function of the molar mass of the grafted polystyrene chains (route I, Table 1).

the access of the propagating radicals in the volume to the living surface polymer. This is in perfect agreement with the results obtained in route I which showed that termination reactions were promoted for low alkoxyamine grafting densities (i.e., for low surface polymer concentrations).

Another interpretation relies on physisorption phenomena involving nonreacted DEPN and/or the alkoxyamine compounds formed in situ. Adsorption is presumed to take place via hydrogen bond formation between the carbonyl or the phosphonyl moieties of the alkoxyamine compound and the silanol groups of silica. These physisorbed molecules are strongly anchored to the surface as they could not be displaced by a series of five centrifugation/redispersion cycles in toluene. However, desorption of these physically adsorbed initiator molecules might occur during polymer chain growth. Indeed, the growing polymer becomes more and more hydrophobic and displays therefore less affinity for the inorganic surface. This will result therefore in decreased initiation efficiency but will not influence the livingness of the polymerization process. According to this hypothesis, the increase of the initiation efficiency with increasing surface alkoxyamine concentration (i.e., grafted



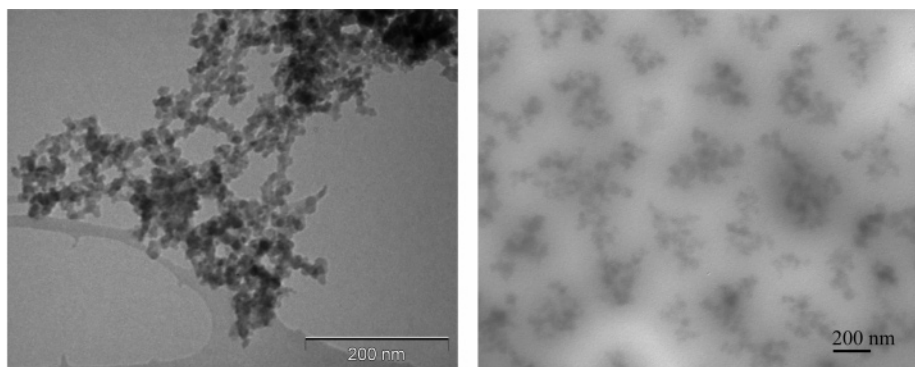


**Figure 8.** TEM images of (a) bare silica particles and (b) PS-grafted silica particles cast from dilute toluene suspensions.  $M_n(\text{PS}) = 60000$  g/mol (route I, sample 4 in Table 1).

plus physisorbed molecules) suggests that the higher the alkoxyamine content on the surface, the lower the proportion of physisorbed species. Previously grafted alkoxyamine molecules may prevent further adsorption of DEPN-based species on the inorganic surface.

**Morphological Characterization.** Insight into the composite particle size and morphology was provided by DLS measurements and TEM analysis. While the original silica particles form aggregates and settle down in toluene, silica particles grafted with polystyrene chains of molecular weights larger than around 20000 form stable colloidal suspensions with a mean diameter comprised between 150 and 190 nm (Table 1). The composite particle diameter increases as the polystyrene chain length increases (Figure 7). These results show that the dispersability and stability of the silica particles in toluene are significantly improved after grafting.

Figure 8 shows the TEM images of the original silica particles and of the nanocomposite sample cast from dilute toluene suspensions. The TEM micrograph of Aerosil shows micrometer-sized domains of stringy-shaped aggregated particles. These agglomerates are partly destroyed after polymerization, and the silica particles appear regularly distributed within the polystyrene film. The silica beads are organized into domains, the size of which is close to the hydrodynamic diameter determined by DLS measurements (Table 1).

## Conclusion

A new convenient procedure is reported that allows the in situ formation of surface-active alkoxyamine compounds in a one-step process. This technique involves the simultaneous reaction of a polymerizable silane (APTMS), a source of radical (AIBN), and a nitroxide free radical (DEPN) used as a spin trap. An optimum alkoxyamine grafting density of around  $0.75 \mu\text{mol}/\text{m}^2$  (based on phosphorus elemental analysis) was reached using this method. This value is slightly lower than the grafting density previously reported for a preformed triethoxysilyl-terminated alkoxyamine initiator. Comparison of elemental analysis with the TGA results together with  $^{13}\text{C}$  solid-state NMR analysis showed that nonreacted APTMS molecules were also present on the surface. The presence of residual APTMS suggests that competitive events occurred during grafting. Polystyrene chains with molecular weights comprised between 30000 and 60000 and narrow polydispersities were successfully grown from the surface of the alkoxyamine-grafted silica nanoparticles. The maximum grafting density of the surface-tethered PS chains was estimated to be around  $0.35 \mu\text{mol}/\text{m}^2$ , which cor-

responds to more than 45% initiation efficiency. The larger the alkoxyamine grafting density, the higher the amount of grafted polystyrene chains, and the larger the fraction of initiator units that effectively participated in the growth reaction. DLS measurements and TEM observations showed that the dispersability of silica in toluene was significantly improved when the molecular weight of the grafted PS chains was larger than around 20000. The polymer formed on the silica surface allowed partial destruction of the agglomerates whose hydrodynamic diameter decreased to around 150 nm.

Work is under way to extrapolate this technique to colloidal silica suspensions to examine the influence of the polymer chain length on the thickness of the polymer layer. The possibility to control nanoparticle ordering and interparticle distance by varying the polymer molecular weight will also be evaluated in this future work.

**Acknowledgment.** We are indebted to Jean-Luc Couturier and Olivier Guerret from Atofina for supplying DEPN. We are very grateful to Christian Novat (Laboratoire de Chimie et Procédés de Polymérisation) for his help in the TEM observations.

**Supporting Information Available:**  $^{29}\text{Si}$ ,  $^{13}\text{C}$ , and  $^{31}\text{P}$  CP-MAS solid-state NMR spectra of the alkoxyamine-functionalized silica particles (second route). This material is available free of charge via the Internet at <http://pubs.acs.org>.

## References and Notes

- (1) For reviews in this field, see: (a) Kroker, R.; Schneider, M.; Hamann, K. *Prog. Org. Coat.* **1972**, *1*, 23–44. (b) Kickelbick, G.; Schubert, U. In *Synthesis, Functionalization and Surface Treatment of Nanoparticles*; Baraton, M.-L., Ed.; American Scientific Publishers: Stevenson Ranch, CA, 2002; Vol. 6, pp 1–12. (c) Kickelbick, G. *Prog. Polym. Sci.* **2003**, *28*, 83–114. (d) Bourgeat-Lami, E. *J. Nanosci. Nanotechnol.* **2002**, *2*, 1–24.
- (2) Prucker, O.; Rühle, J. *Macromolecules* **1998**, *31*, 592–601.
- (3) Prucker, O.; Rühle, J. *Macromolecules* **1998**, *31*, 602–613.
- (4) Prucker, O.; Rühle, J. *Langmuir* **1998**, *14*, 6893–6898.
- (5) (a) Ryan, K. *Chem. Ind.* **1988**, *6*, 359–364. (b) Krenkler, K. P.; Laible, R.; Hamann, K. *Angew. Makromol. Chem.* **1976**, *53*, 101–123.
- (6) (a) Zhou, Q.; Wang, S.; Fan, X.; Advincula, R.; Mays, J. *Langmuir* **2002**, *18*, 3324–3331. (b) Quirk, R. P.; Mathers, R. T. *Polym. Bull.* **2001**, *45*, 471–477.
- (7) Tsubokawa, N.; Kimoto, T.; Endo, T. *Polym. Bull.* **1994**, *33*, 187–194.
- (8) Joubert, M.; Delaite, C.; Bourgeat-Lami, E.; Dumas, P. *J. Polym. Sci., Part A: Polym. Chem.* **2004**, *42* (8), 1976–1984.
- (9) Hawker, C. J.; Barclay, G. G.; Orellana, A.; Dao, J.; Devonport, W. *Macromolecules* **1996**, *29*, 5245–5254.

- (10) (a) Devaux, C.; Beyou, E.; Chapel, J. P.; Chaumont, P. *Eur. Phys. J.* **2002**, *7*, 345–352. (b) Tomlinson, M. R.; Genzer, J. *Macromolecules* **2003**, *36*, 3449–3451. (c) Husseman, M.; Malmström, E. E.; McNamara, M.; Mate, M.; Mecerreyes, D.; Benoit, D.; Hedrick, J. L.; Mansky, P.; Huang, E.; Russel, T. P.; Hawker, C. J. *Macromolecules* **1999**, *32*, 1424–1431.
- (11) (a) von Werne, T.; Patten, T. E. *J. Am. Chem. Soc.* **2001**, *123*, 7497–7505. (b) Tsujii, Y.; Ejaz, M.; Sato, K.; Goto, A.; Fukuda, T. *Macromolecules* **2001**, *34*, 8872–8878. (c) Matsuno, R.; Yamamoto, K.; Otsuka, H.; Takahara, A. *Chem. Mater.* **2003**, *15*, 3–5. (d) Matsuno, R.; Yamamoto, K.; Otsuka, H.; Takahara, A. *Macromolecules* **2004**, *37*, 2203–2209.
- (12) Böttcher, H.; Hallensleben, M. L.; Nu, S.; Wurm, H. *Polym. Bull.* **2000**, *44*, 223–229.
- (13) Ohno, K.; Koh, K.; Tsujii, Y.; Fukuda, T. *Macromolecules* **2002**, *35*, 8989–8993.
- (14) (a) Moad, G.; Rizzardo, E.; Solomon, D. H. *Macromolecules* **1982**, *15*, 909–914. (b) Veredin, R. P. N.; Georges, M. K.; Hamer, G. K.; Kazmaier, P. M. *Macromolecules* **1995**, *28*, 4391–4398. (c) Hawker, C. J. *Trends Polym. Sci.* **1996**, *4*, 183–X. (d) Catala, J. M.; Bubel, F.; Hammouch, S. O. *Macromolecules* **1995**, *28*, 8441–8443. (e) Hammouch, S. O.; Catala, J. M. *Macromol. Rapid Commun.* **1996**, *17*, 149–154. (f) Bralau, R.; Burrill, L. C.; Siano, M.; Naik, N.; Hoden, R. K.; Mahal, L. K. *Macromolecules* **1997**, *30*, 6445–6450. (g) Matyjaszewski, K.; Shigemoto, T.; Frechet, J. M.; Leduc, M. *Macromolecules* **1996**, *29*, 4167–4171. (h) Shigemoto, T.; Matyjaszewski, K. *Macromol. Rapid Commun.* **1996**, *17*, 347–351. (i) Benoit, D.; Grimaldi, S.; Finet, J. P.; Tordo, P.; Fontanille, M.; Gnanou, Y. *J. Am. Chem. Soc.* **2000**, *122*, 5929–5939.
- (15) Hawker, C. J. *J. Am. Chem. Soc.* **1994**, *116*, 11185–11186.
- (16) For a review in this field, see: Hawker, C. J.; Bosman, A. W.; Harth, E. *Chem. Rev.* **2001**, *101*, 3661–3688.
- (17) Blomberg, S.; Ostberg, S.; Harth, E.; Bosman, A. W.; van Horn, B.; Hawker, C. J. *J. Polym. Sci., Part A: Polym. Chem.* **2002**, *40*, 1309–1320.
- (18) (a) Parvole, J.; Laruelle, G.; Guimon, C.; François, J.; Billon, L. *Macromol. Rapid Commun.* **2003**, *24*, 1074–1078. (b) Laruelle, G.; Parvole, J.; François, J.; Billon, L. *Polymer* **2004**, *45*, 5013–5020.
- (19) Bartholome, C.; Beyou, E.; Bourgeat-Lami, E.; Chaumont, P.; Zydowicz, N. *Macromolecules* **2003**, *36*, 7946–7952.
- (20) Beyou, E.; Humbert, J.; Chaumont, P. *e-Polymers* **2003**, 020.
- (21) Parvole, J.; Billon, L.; Montfort, J. P. *Polym. Int.* **2002**, *51*, 1111–1116.
- (22) Kasseh, A.; Ait-Kadi, A.; Riedl, B.; Pierson, J. F. *Polymer* **2003**, *44*, 1367–1375.
- (23) (a) Bourgeat-Lami, E.; Lang, J. J. *Colloid Interface Sci.* **1998**, *197*, 293–308. (b) Bourgeat-Lami, E.; Lang, J. J. *Colloid Interface Sci.* **1999**, *210*, 281–289. (c) Corcos, F.; Bourgeat-Lami, E.; Novat, C.; Lang, J. *Colloid Polym. Sci.* **1999**, *277*, 1142–1151.
- (24) Reculosa, S.; Mingotaud, C.; Bourgeat-Lami, E.; Duguet, E.; Ravaine, S. *Nano Lett.* **2004**, *4*, 1677–1682.
- (25) Couturier, J. L.; Guerret, O. PCT Int. Appl. WO 0212149, 2002.
- (26) Koppel, D. E. *Chem. Phys.* **1972**, *57*, 4814–4820.
- (27) Bauer, F.; Freyer, A.; Ernst, H.; Gläsel, H.-J.; Mehnert, R. *Appl. Surf. Sci.* **2001**, *179*, 119–122.
- (28) Bourgeat-Lami, E.; Espiard, P.; Guyot, A. *Polymer* **1995**, *36*, 4385–4389.
- (29) Ananchenko, G.; Marque, S.; Gigmes, D.; Bertin, D.; Tordo, P. *Org. Biomol. Chem.* **2004**, *2*, 709–715.
- (30) Since the coupling reaction is conducted at a temperature lower than the alkoxyamine activation temperature, the AIBN radicals are no longer available for addition to the APTMS double bonds.
- (31) von Werne, T.; Patten, T. E. *J. Am. Chem. Soc.* **1999**, *121* (32), 7409–7410.
- (32) Pyun, J.; Kowalewski, T.; Matyjaszewski, K. *Macromol. Rapid Commun.* **2003**, *24*, 1043–1059.

MA048501I